JOURNAL OF MATERIALS SCIENCE 11 (1976) 2061–2067

A new source of X-ray line broadening: inhomogeneous strains induced by uniform homogeneous temperature conditions in polyphase or non-cubic materials

FRANKLIN H. COCKS, STUART F. COGAN
Department of Mechanical Engineering and Materials Science, Duke University, Durham, North Carolina, USA

Thermal strains may contribute to X-ray diffraction line broadening in both single-phase non-cubic and in polyphase cubic polycrystalline materials even under uniform temperature conditions. A method is developed for calculating the magnitude of these thermally induced strains directly from the measured diffraction peak profiles. Corrections for particle-size effects can be made readily if particle-size broadening is significant, and the thermal diffuse scattering (TDS) contribution to the diffracted intensity can be taken into account experimentally. By this method, the strains in a Mg–5 wt% Si alloy were found to be increased by as much as 35% by a 190° C temperature change. Even in the case of this relatively low melting point alloy, the TDS effect causes only a maximum of 15% error in these measured strain effects. The interpretation of these isothermally induced strains in terms of crystal anisotropy, grain morphology and orientation and the relative sizes of phases and grains is discussed.

1. Introduction

In single crystals of all kinds, in isotropic amorphous materials, and in polycrystalline substances of cubic symmetry, thermal stresses can be generated only by temperature gradients. In polycrystalline aggregates of materials with less than cubic symmetry, however, strains will be induced even if the temperature is entirely uniform and temperature gradients do not exist. These strains arise because of the anisotropic variation in thermal expansion coefficient within these materials. A change in the uniform temperature condition will alter the magnitude of such thermal strains. Thermal strains will also occur in materials such as composites and eutectic systems where a plurality of phases exhibit different thermal expansion coefficients. Although many studies have been made of thermal stresses and thermal fatigue induced by temperature gradiants, there have only been a few studies of those stresses induced by uniform homogeneous temperatures and the possible fatigue which may arise during thermal cycling of non-cubic polycrystalline materials. Early investigations have shown that such thermal fatigue in non-cubic metals can cause extensive deformation and cracking even under modest thermal cycling rates [1–3].

For two-phase materials, Malygin and Likhachev [4] have listed a number of temperature-induced stress values for particular metals embedded in other metallic matrices having different coefficients of thermal expansion. The actual induced stress for a temperature of 1° C, may be as high as 526 psi*, as in the case of silver embedded in platinum. Likhachev [5] has developed solutions for the expected thermally induced stress in single-phase anisotropic materials for all 32 crystal classes. In the present work, an X-ray line-broad-

* 10^3 psi $\equiv$ 6.89 N mm^{-2}.

ening method has been developed which permits the quantitative and direct experimental determination of the inhomogeneous localized strains which can be produced in non-cubic or polyphase materials by uniform temperature changes.

X-ray line broadening measurements have in the past been used extensively to measure particle size and microstructural strains, particularly as a result of cold-working [6, 7]. A significant difficulty with this method has been associated with the need to separate line broadening effects due to particle size from those due to strain. If the strain is produced thermally and not mechanically, however, then there will be no change in the particle-size effect on the line broadening, unless very extensive twinning or slip were to occur. However, in almost all cases, deformation will not occur unless a large number of thermal cycles are used [1]. As will be shown, when allowance for the effect of thermal diffuse scattering (TDS) on intensity is made, it is possible to obtain the temperature-induced change in microstructural strains directly, without complications from the particle-size effect. In the following section, the theoretical development of our approach is reviewed, and it is shown how TDS effects may be readily taken into account experimentally.

2. Theory

For crystalline materials with two or more discernable phases with differing coefficients of thermal expansion, and for single-phase polycrystalline materials with less than cubic symmetry, changes in temperature will cause localized strains. These strains are a result of the difference in the bulk thermal expansion coefficients of the phases or the variation in thermal expansion coefficient, with crystallographic direction, of the non-cubic material.

Two distinct types of thermal strains may occur. First, bulk strain, as measured by the shift of the X-ray diffraction peak, represents the change in the average interplanar spacing as a result of variation in temperature. The actual observed bulk strain will be predicted by the thermal expansion coefficients of the phases involved. The second type of thermal strain, the induced microstrain or r.m.s. strain, causes a broadening of the diffraction peak. This results from the fact that each crystallite will not, as a rule, see the average or polycrystalline expansion coefficient and modulus of the material around it.

One difficulty in obtaining the r.m.s. strain from the measured line broadening is the effect of TDS on the intensity and shape of the diffraction peak [8, 9]. At lower temperatures where the TDS contribution is less the diffraction peaks tend to be narrower and of a higher maximum intensity than peaks at ambient temperatures. As the temperature is lowered, therefore, the TDS tends to sharpen line profiles, while inhomogeneous strain effects will, in general, tend to broaden the profile. Values for the temperature-induced r.m.s. strain that are free of TDS may, however, be obtained by unfolding, using the method of Stokes [10], both high and low temperature peaks against strain-free profiles of the same material at corresponding temperatures.

The four peak profiles necessary to obtain the r.m.s. strain and to correct experimentally for TDS effects are shown schematically in Fig. 1. Profiles 1 and 2 are the room temperature and low temperature profiles of the massive block sample, whilst profiles 3 and 4 are the profiles of the corresponding strain-free powdered specimens. Profile 1 is unfolded with respect to profile 3 and profile 2 is unfolded with respect to profile 4 to obtain the strain profiles of the massive block specimen at the two given temperatures, and to eliminate any TDS and instrumental broadening which may be present. A direct comparison of the r.m.s. strain present at each temperature as calculated from these resolved profiles will then yield directly the actual change in the r.m.s. strain induced over the given temperature range. The simplest way of producing the strain-free specimens needed at each temperature, is through the use of powdered specimens mounted using a medium which will not itself cause strain during cooling or heating [11].

Resolution of the broadened profile against its appropriate powdered sample reference profile will now produce profiles which contain only particle size and strain effects. It is unlikely that, in massive bulk samples, particle-size effects will be significant. For a particle size greater than about 5000 to 10000 Å there is a negligible contribution. However, when particles are less than 2000 Å, it is necessary to remove the particle-size contribution. This separation of particle size and strain effects can be carried out using the multiple-order method of Warren and Averbach [6, 7], or the single-line technique of Smith [12] and Mitra and co-workers [13, 14]. The average

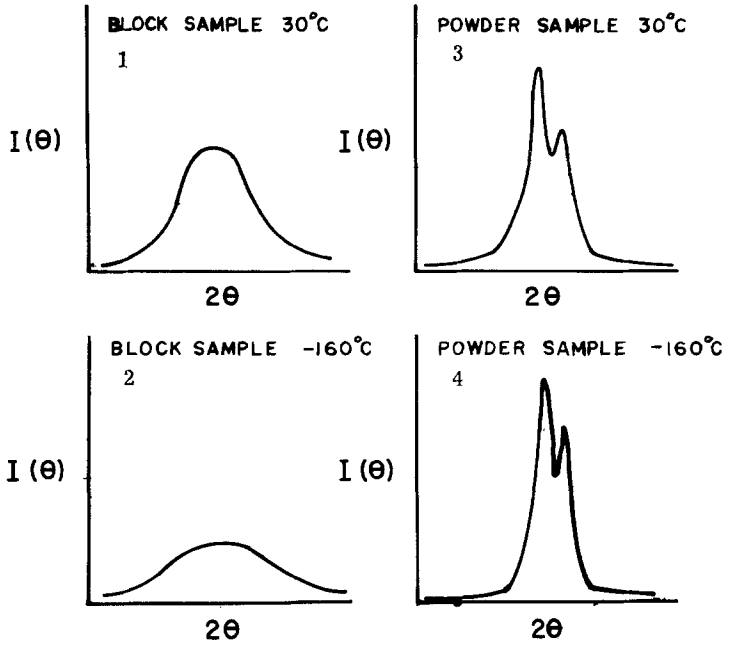

Figure 1 The four diffraction peak profiles necessary to determine the temperature induced r.m.s. strain independently of any TDS effects. The room temperature block profile, 1, low temperature block profile, 2, room temperature powder profile, 3, and low temperature powder profile, 4, are unfolded 1 against 3 and 2 against 4.

particle size, $\bar{N}$, as evaluated by Warren and Averbach [6] and Bertaut [15] is given by

$$\frac{\mathrm{d}}{\mathrm{d}L}\left(\frac{A_L}{A_0}\right)_{L=0} = \frac{1}{\bar{N}}, \tag{1}$$

where A_L is the Fourier coefficient of the resolved diffraction peak as a function of the index L, normalized such that $A_0 = 1$, and $\bar{N}$ is the average particle size. The index L is the distance normal to the reflecting planes, given by $L = na_3$, where n is the harmonic number of the Fourier coefficients and a_3 is the distance between the reflecting planes modified by the Fourier interval in which the peak is measured. This parameter is evaluated from $a_3 = \lambda/[4(\sin\theta - \sin\theta_0)]$. The term $\sin\theta - \sin\theta_0$ is the half interval over which the peak is measured, where θ_0 is the angle of the peak maximum and θ is the angle of the peak termination at one side of this assumed symmetrical peak maximum. Since the expression in Equation 1 is simply the slope of the plot of the normalized coefficients versus L, as L tends to zero, the average particle size can readily be evaluated. The particle-size coefficients, A_L^{P} for each value of L, are then obtained from [14]:

$$A_L^{\mathrm{P}} = 1 - \frac{L}{\bar{N}} \tag{2}$$

and the strain coefficients, A_L^{S} are then evaluated from the well-known expression,

$$A_L = A_L^{\mathrm{P}} A_L^{\mathrm{S}}. \tag{3}$$

Since we expect the average particle size to be significantly greater than 2000 Å, the normalized particle size coefficients obtained from Equation 2 should be close to unity.

In the general case, the strain coefficients are related to the strain for low orders of a given reflection and index L(e.g. $l < 4$ if $Z_L = 0.05$) by [16]:

$$A_L^{\mathrm{S}} = \exp(-2\pi^2 l^2 \langle Z_L^2 \rangle) \tag{4}$$

where $\langle Z_L^2 \rangle$ is the average squared relative displacement of the reflective planes. Equation 4 is correct for any general reflection $(h\,k\,l)$ regardless of the crystal system, the result being identical with that obtained when the strain is evaluated from consideration of the $(0\,0\,l)$-type reflection only [16]. The component of the strain measured in a direction perpendicular to the reflecting planes ϵ_L, is given by $\epsilon_{\mathrm{L}} = Z_{\mathrm{L}}/n$ and is the strain averaged over the distance $L = a_3 n$. The r.m.s. strain may then be plotted against distance in the direction perpendicular to the reflecting planes being examined, for both high and low temperature strain states. The manner by which the strains are calculated is

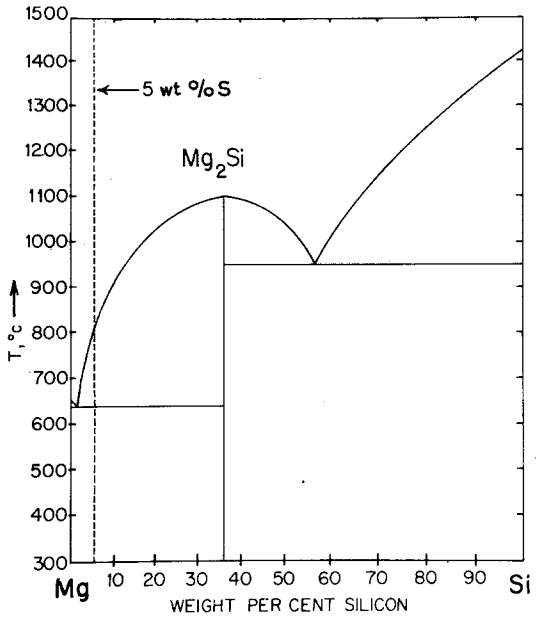

Figure 2 The phase diagram of the Mg–Si system [23]. The composition of the alloy used in this investigation is shown by the dotted line.

independent of any assumptions concerning the distribution of strain other than the fact that the expression in Equation 4 is a Taylor series expansion of $\cos\langle 2\pi lZ\rangle$ and requires that the higher order terms are small [17].

3. Experimental procedure

The experiments were conducted using a Mg–5 wt% Si alloy. This alloy consists at equilibrium of a matrix of pure magnesium with particles of Mg_2Si embedded in the matrix, as may be seen from the Mg–Si phase diagram shown in Fig. 2. The Mg–Si alloy was prepared by melting high purity magnesium and silicon under a flux of KCl (62 wt%) and $MgCl_2$ (38 wt%) to prevent burning and oxidation. The melt was cast into moulds which were coated with a thin layer of sulphur to further prevent deterioration of the magnesium. The sample used in the line-broadening analysis was sectioned from the centre of the cast ingot, and found by X-ray analysis to contain no residual silicon. The massive block samples obtained in the above manner were polished with 0.3 μm alumina to a thickness of 0.3 mm. The powder samples were prepared from Mg_2Si* comminuted to a −400 mesh powder, and mounted so that no strain would be produced during cooling [11]. The as-cast massive block samples were cold-worked 3.5% and then annealed for over 2 h at 300° C, in order to reduce any line-broadening effects of the residual cold-work prior to the line-broadening measurements.

The line-broadening measurements were carried out using a General Electric XRD-5 diffractometer with Ni-filtered Cu$K\alpha$ (1.5418 Å) radiation. Providing good alignment of the diffractometer and resolution are employed, separation of the $K\alpha$ doublet is unnecessary [18]. The (2 2 0) reflections of the Mg_2Si precipitates in the massive block sample and in the powdered sample were analysed by point counting at both 30° C and at −160° C. The time required to accumulate 1000 counts, with a probable error of 2.1%, was measured at intervals of 0.02° in 2θ across the peak profile, and the Fourier coefficients of the resultant diffraction peak profile, were evaluated using a computer program designed specifically for this type of X-ray analysis [19].

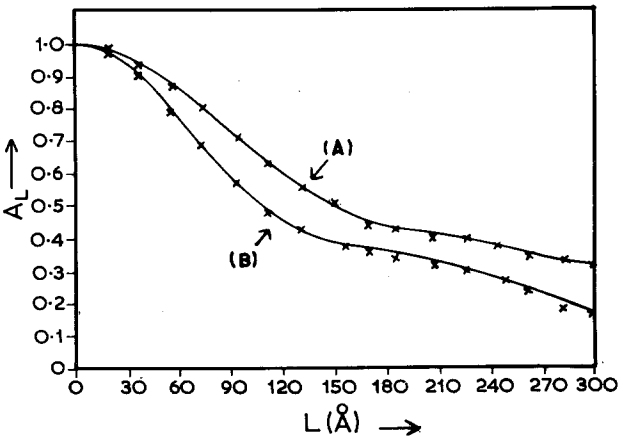

Figure 3 The Fourier coefficients A_L corrected for instrumental broadening. These coefficients contain both strain and particle size effects. They are shown plotted against a distance, L, normal to the (2 2 0) reflecting planes for both the, 30° C curve A, and the −160° C curve B, peak profiles.

* Obtained from Cerac Corporation, Box 1178, Milwaukee Wisconsin 53201, USA.

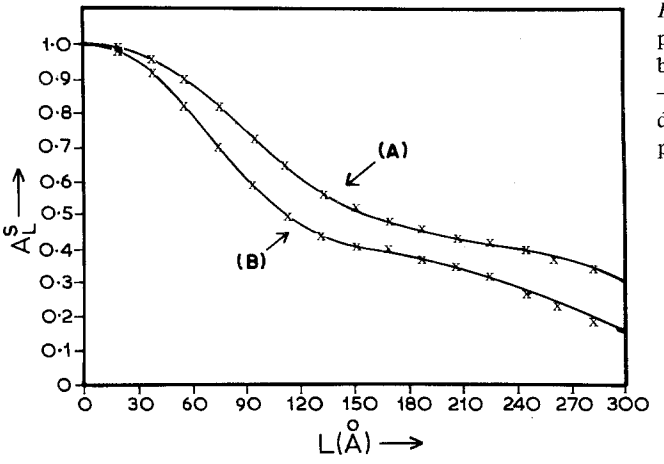

Figure 4 The Fourier coefficients, corrected for particle size effects, representing the strain broadening only for the 30° C curve A, and −160° C curve B, peak profiles plotted against distance, L, normal to the (2 2 0) reflecting planes.

4. Results

The profiles of the (2 2 0) Mg_2Si reflection obtained from the massive block sample at 30° C and −160° C were corrected for instrumental broadening by resolving against the Mg_2Si powder peak profiles at these same temperatures. The coefficients of the resultant peaks, free from instrumental-broadening and TDS effects, represent solely the strain and particle-size contributions to the line broadening and are shown in Fig. 3. From the initial slopes of the plots of these coefficients the average particle size for the Mg_2Si phase was obtained, and found to be about 5000 Å, at both temperatures, and hence contributed only marginally to the measured line broadening. From the average particle size, and Equation 2, the particle-size coefficients were calculated and used to correct the peak profiles for any residual particle-size broadening. The coefficients representing purely the strain-broadening contribution are shown in Fig. 4. The marked decrease in the low temperature coefficients is strongly reflected in the higher strain state for that temperature (Fig. 5). It can be seen that a change in temperature of the block sample from 30° C to −160° C has increased the r.m.s. microstrains by some 35% over the first 100 Å, corresponding to an average absolute change in strain of approximately 0.34%. The fact that the room temperature strain profile shows a considerable amount of residual strain in the Mg_2Si phase, which was not annealed out after cold-working, indicates that the effect of isothermal strains in a fully annealed sample might be even greater.

The change in the r.m.s. strain, independent of any TDS, can be seen as the difference between curves A and B in Fig. 5. This difference is also shown directly as curve A in Fig. 6. The magnitude of the TDS effect can be measured by evaluating the change in strain profile obtained from unfolding the low temperature block sample, peak 2 Fig. 1, against the room temperature powder

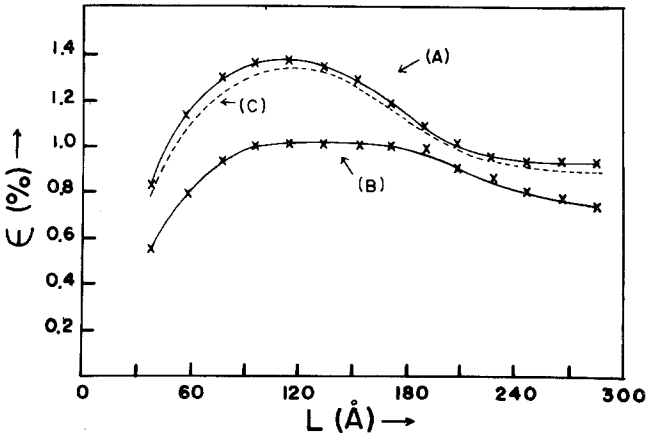

Figure 5 The r.m.s. Strains at 30° C, curve B, and −160° C, curve A, calculated from the coefficients in Fig. 4 and the r.m.s. strain without TDS correction dashed curve C, plotted against distance, L, normal to the reflecting planes.

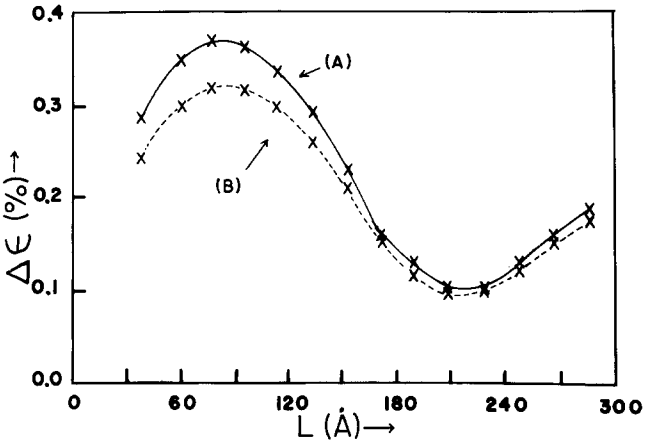

Figure 6 A comparison of the change in the r.m.s. strain computed (A) with the TDS contribution experimentally removed and (B) from the direct unfolding of the profiles of the low temperature massive block sample and the high temperature powder sample. The differences in the calculated strain changes caused by TDS effects are approximately 15% or less.

sample, peak 3 Fig. 1. The room temperature strain profile, curve B Fig. 5, can then be subtracted and the result compared with the change in strain determined independently of the TDS, curve A Fig. 6. By this method the maximum correction for the TDS effect was 15%. The change in strain determined without correction for TDS is shown in Fig. 6, curve B. As expected, such uncorrected strains are always found to be less than the change in strain calculated taking TDS into account. The room temperature block profile is thus slightly broader than it would be if the TDS were not present. Of course, if sufficient data were available, the TDS effect could also be estimated theoretically [8, 9].

It is important to note that the strain induced by uniform homogeneous temperature conditions will depend not only on the modulii and thermal expansion coefficients of Mg and Mg_2Si, but also on the relative size and dispersion of the Mg_2Si grains in the surrounding Mg matrix. Previous order of magnitude estimates of the induced stresses in anisotropic materials have been carried out by Boas and Honeycombe [1] who considered a linear boundary element between two grains of modulli E_1 and E_2 and thermal expansion coefficients α_1 and α_2. If we incorporate the widths of the grains W_1 and W_2 into their expression for the induced stress, then for a given drop in temperature, ΔT, the average induced stress in the grain of width W_2 would be

$$\sigma_2 = \left(\frac{E_1 E_2 W_1}{W_2 E_2 + W_1 E_1}\right)(\alpha_2 - \alpha_1)\Delta T. \quad (5)$$

Representing Mg by subscript 1 and Mg_2Si by subscript 2 we have, for the (2 2 0) reflection of the Mg_2Si [20, 21] that $E_2 = 11.9 \times 10^{10}\,N\,m^{-2}$ and $\alpha_2 = 7.7 \times 10^{-6}\,^\circ C^{-1}$ (as determined from present powder peak position measurements from 30° C to −160° C). For polycrystalline magnesium, $E_1 = 4.5 \times 10^{10}\,N\,m^{-2}$ and $\alpha_1 = 25.5 \times 10^{-6}\,^\circ C^{-1}$. If the ratio of the widths W_1/W_2 is varied from 0.1 to 20.0 then the stress in the Mg_2Si grain will vary from $1.4 \times 10^7\,N\,m^{-2}$ to $1.7 \times 10^8\,N\,m^{-2}$ and the induced strain will vary from 0.012% to 0.30%. These are, of course, only approximations to actual conditions, but serve to show that variations in grain morphology may be a factor contributing to strain broadening. The method of Likhachev [5], who considers a grain totally embedded in a rigid matrix, gives values for induced stresses which are, on the whole, 1/2 to 1/3 of those as calculated by Boas and Honeycombe. But even Likachev did not make an allowance for the variation in relative sizes of adjacent grains.

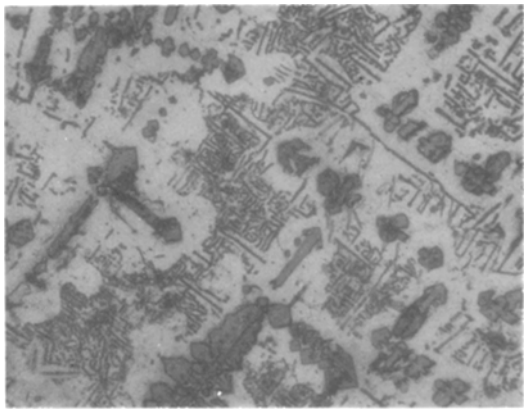

Figure 7 Photomicrograph of the 95 wt% Mg– 5 wt% Si alloy showing the variation in morphology of the Mg_2Si precipitates. The larger precipitates are the proeutectic Mg_2Si whilst the smaller lamellar-like structures are the eutectic Mg_2Si (etched in 2% nital, × 200).

The photomicrograph of the Mg–5 wt% Si block sample (Fig. 7) shows the existence of two distinct grain morphologies. The larger grains constitute the proeutectic Mg_2Si, whilst the much smaller elongated grains are the eutectic Mg_2Si. It is important to consider the dispersion and relative dimensions of the grains particularly, as shown in Fig. 7, when distinct grain morphologies exist. The strain broadening that these grains exhibit will depend critically upon their depth below the sample surface and the distance between grains. Variations in strain will occur because the dimensions of the adjacent grains are varied and a variety of different strain states exist, all contributing to the line broadening. It may be that for structures in which the eutectic grains have definite directional properties, or some preferred habit, particular crystallographic directions may exhibit a significant contribution to strain broadening. In any case, regardless of particle-size dispersion, relative modulii, and relative thermal expansion coefficients, the method developed in the present work will quantitatively measure the thermally induced inhomogeneous strain.

5. Conclusion

Thermally induced strains may contribute to line broadening in multi-phase polycrystalline materials or in single-phase polycrystalline material where the phase present possesses symmetry of lower order than cubic. In polyphase materials, such strain effects will occur even if all phases are cubic provided that the thermal expansion coefficients of the various phases are different. The observed strain will also be influenced by the dispersion of grains and the grain morphology, through the variation in relative lengths of adjacent grains.

In the case of a Mg–5 wt% Si alloy examined, strains were found to increase some 35% over a temperature range from 30° C to −160° C and were measured by means of the X-ray broadening effects which such strains produced. Not only will this method yield the actual change in strain, but will also give an indication of the strain profile, or change in strain profile, over small domains in the material examined.

An approximate indication as to whether or not a material will exhibit line broadening as a result of uniform temperature changes can be obtained from an examination of the crystal class, modulus and thermal expansion coefficient. In addition, relative physical sizes and size dispersion of the phases present, may also contribute to the development of inhomogeneous strains [22].

Acknowledgements

We wish to thank Dr Robert M. Rose, of the Massachusetts Institute of Technology, for allowing us the use of his low temperature X-ray cryostat, and Dr C. P. Gazzara of the Army Mechanics and Materials Research Center, Watertown, Mass, for providing us with a copy of his Unfold Computer Program.

References

1. W. BOAS and R. W. K. HONEYCOMBE, *Proc. Roy. Soc.* **186A** (1946) 57.
2. *Idem, ibid* **188A** (1946/47) 427.
3. *Idem, J. Inst. Metals* **73** (1946/47) 433.
4. G. A. MALYGIN and V. A. LIKHACHEV, *Zavodskaya Laboratoriya* **32** (3) (1966) 335.
5. V. A. LIKHACHEV, *Sov. Phys. Solid State* **3** (1961) 1330.
6. B. E. WARREN and B. L. AVERBACH, *J. Appl. Phys.* **21** (1950) 595.
7. B. E. WARREN, *Prog. Met. Phys.* **8** (1959) 147.
8. D. R. CHIPMAN and A. PASKIN, *J. Appl. Phys.* **30** (1959) 1992.
9. D. R. CHIPMAN and C. B. WALKER, *Acta Cryst.* **A28** (1972) 572.
10. A. R. STOKES, *Proc. Phys. Soc.* **61** (1948) 382.
11. F. H. COCKS and S. F. COGAN, *J. Appl. Cryst.* 8 (1975) 571.
12. R. S. SMITH, *IBM J. Res. and Dev.* 4 (1960) 205.
13. G. B. MITRA and N. K. MISRA, *Acta Cryst.* **22** (1967) 454.
14. G. B. MITRA and A. K. CHAUDHURI, *J. Appl. Cryst.* 7 (1974) 350.
15. M. F. BERTAUT, *Compt. Rend. Acad. Sci. Paris* **228** (1949) 492.
16. B. E. WARREN, *Acta Cryst.* 8 (1955) 483.
17. B. E. WARREN, "X-Ray Diffraction" (Addison-Wesley, Reading, Mass., 1969).
18. A. KIDRON and J. B. COHEN, *J. Appl. Cryst.* **6** (1973) 8.
19. C. P. GAZZARA, J. J. STIGLICH, F. P. MEYER and A. M. HANSEN, *Adv. X-Ray Anal.* **12** (1968) 257.
20. A. B. DAYAI, *J. Phys. C. Solid State Phys.* **3** (1970) 2037.
21. W. B. WHITTEN, P. L. CHUNG and G. C. DANIELSON, *J. Phys. Chem. Solids* **26** (1965) 49.
22. F. H. COCKS, C. N. PREECE and H. W. KING, *Phys. Letters* **22** (1966) 287.
23. M. HANSEN, "Constitution of Binary Alloys" McGraw-Hill, New York, 1958).

Received 23 January and accepted 3 May 1976.